01 Nov 1994

A Magnetic, Neutron Diffraction, and Mössbauer Spectral Study of the $Nd_2Fe_{17-x}Al_x$ Solid Solutions

Gary J. Long
Missouri University of Science and Technology, glong@mst.edu

Gaya Kanishka Marasinghe

Sanjay R. Mishra

Oran Allan Pringle
Missouri University of Science and Technology, pringle@mst.edu

et. al. For a complete list of authors, see https://scholarsmine.mst.edu/chem_facwork/768

Recommended Citation

G. J. Long et al., "A Magnetic, Neutron Diffraction, and Mössbauer Spectral Study of the $Nd_2Fe_{17-x}Al_x$ Solid Solutions," *Journal of Applied Physics*, vol. 76, no. 9, pp. 5383-5393, American Institute of Physics (AIP), Nov 1994.
The definitive version is available at https://doi.org/10.1063/1.357193

A magnetic, neutron diffraction, and Mössbauer spectral study of the $Nd_2Fe_{17-x}Al_x$ solid solutions

Gary J. Long
Department of Chemistry, University of Missouri-Rolla, Rolla, Missouri 65401-0249

G. K. Marasinghe, S. Mishra, and O. A. Pringle
Department of Physics, University of Missouri-Rolla, Rolla, Missouri 65401-0249

Z. Hu and W. B. Yelon
University of Missouri Research Reactor and the Departments of Chemistry and Physics, University of Missouri-Columbia, Columbia, Missouri 65211

D. P. Middleton and K. H. J. Buschow[a)]
Philips Research Laboratories, P.O. Box 80000, NL-5600 JA Eindhoven, The Netherlands

F. Grandjean
Institute of Physics, B5, University of Liège, B-4000 Sart-Tilman, Belgium

(Received 24 March 1994; accepted for publication 7 July 1994)

The magnetic properties of a series of $Nd_2Fe_{17-x}Al_x$ solid solutions, with x equal to 2.04, 4.01, 5.97, 7.94, and 9.06, have been studied by magnetic measurements, neutron diffraction, and Mössbauer spectroscopy. Magnetization studies indicate that the Curie temperature increases from 330 K in Nd_2Fe_{17} to a maximum of ~470 K at an x of 3.5. The compounds crystallize in the Th_2Zn_{17} structure with lattice parameters and unit cell volumes which increase linearly with increasing aluminum content. The neutron diffraction results indicate that aluminum atoms are excluded from the $9d$ site, prefer the $18h$ site at low aluminum content, and prefer the $6c$ and $18f$ sites at high aluminum content. At 10 K the magnetic moments of the iron and neodymium atoms are collinear and take up a basal orientation at all aluminum contents. The moments decrease with increasing aluminum content and the magnetic moments per unit cell at 10 K are in excellent agreement with the 4.2 K saturation magnetization values. At 295 K the $Nd_2Fe_{17-x}Al_x$ solid solutions for x equal to 7.94 and 9.06 are paramagnetic. The magnetic Mössbauer spectra have been fit with a binomial distribution of the near-neighbor environments. The weighted average isomer shift increases, as expected, with increasing aluminum content as a result of interatomic charge transfer and intraatomic iron $4s-3d$ charge redistribution. The weighted average maximum hyperfine field at 295 K shows a maximum of 221 kOe at x equal to 2.04 but at 85 K it decreases uniformly with increasing aluminum content. The weighted average decremental field, ΔH, the change in the hyperfine field per aluminum near-neighbor, decreases with increasing aluminum content. It is proposed that, as a consequence of the increase in the average distance between an iron atom and its next near-neighbor shell with increasing aluminum content, the wavelength of the Friedel oscillation increases and the ratio of this wavelength and the shell distance becomes more favorable for ferromagnetic exchange.

I. INTRODUCTION

When R_2Fe_{17} rare-earth intermetallic compounds are interstitially carbided[1] or nitrided,[2,3] to form $R_2Fe_{17}C_x$ or $R_2Fe_{17}N_x$, their unit cell volumes[4–6] expand by approximately 5% to 7% and, as a result, their Curie temperatures increase by approximately 400°. Because of this increase, these new interstitial materials may form the basis for efficient new permanent magnets. However, the presence of the interstitial carbon or nitrogen causes difficulties[7] in the manufacture of these new magnetic materials. Hence, it is important to search for other means of increasing the unit cell volumes and the Curie temperatures of the R_2Fe_{17} intermetallic compounds. One important approach for doing this is the formation of pseudobinary materials, such as $R_2Fe_{17-x}M_x$, where M is an element which will substitute on one or more of the iron lattice sites and, in so doing, increase the unit cell volume. Possible candidates[8] for M include aluminum, silicon, and gallium, and we have recently reported[9] a dramatic increase in the Curie temperatures of the $Tb_2Fe_{17-x}Ga_x$ solid solutions. The maximum Curie temperature is ~560 K for $Tb_2Fe_{13}Ga_4$. The addition of gallium to Tb_2Fe_{17} is accompanied by a linear increase in the unit cell volume of 8 Å^3 per gallium for x between 1 and 8.

We have also recently reported[10] on the magnetic properties of $R_2Fe_{17-x}Al_x$ where R is Y, Ce, Tb, Dy, Ho, Er, and Tm. In order to better understand these magnetic properties it is particularly important to know the location of the substitutional atom within the iron lattice and we have recently reported that both aluminum[11] and gallium[9] are not randomly distributed over the four crystallographic iron sites but rather

[a)]Present address: Van der Waals-Zeeman Laboratory, University of Amsterdam, NL-1018 XE Amsterdam, The Netherlands.

 0021-8979/94/76(9)/5383/11/$6.00

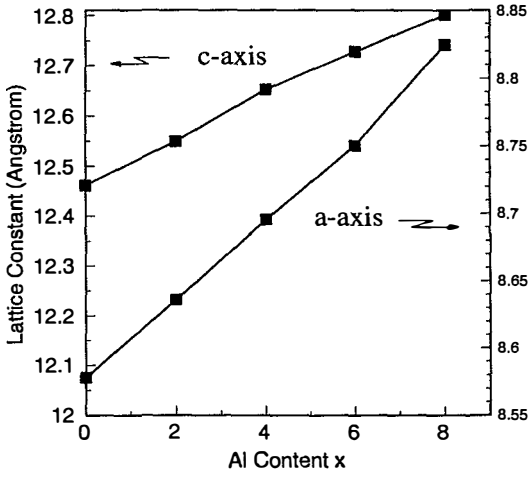

FIG. 1. The compositional dependence of the a and c lattice parameters in the $Nd_2Fe_{17-x}Al_x$ solid solutions.

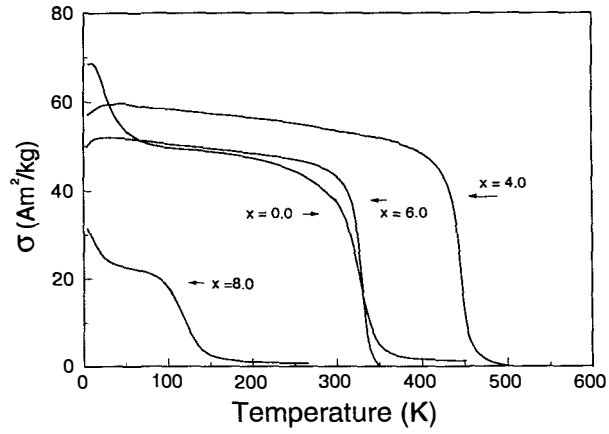

FIG. 2. The temperature dependence of the magnetization measured in a 0.1 T magnetic field of several $Nd_2Fe_{17-x}Al_x$ solid solutions.

are concentrated on specific sites and excluded from other sites.

In this article, we report a detailed magnetic, neutron diffraction, and Mössbauer spectral study of the structural and magnetic properties of $Nd_2Fe_{17-x}Al_x$ at both room and low temperature. We find that the specific site occupancies of the aluminum are important in understanding how the exchange pathway changes in these solid solutions, brought upon by bond length changes affect the long range magnetic ordering. It is interesting that for the $Nd_2Fe_{17-x}Al_x$ solid solutions the increase in Curie temperature is, as expected, accompanied by a unit cell expansion, but such an expansion does not have to occur, as is the case[12] for $Nd_2Fe_{17-x}Si_x$.

II. EXPERIMENTAL METHODS

The samples were prepared from 99.9% pure elements by arc melting. The samples were then annealed at 900 °C for more than three weeks and their phase purity was checked by x-ray diffraction with Cu K_α radiation on a Philips PW 1800/10 x-ray diffractometer equipped with a single crystal graphite monochromator. The $Nd_2Fe_{17-x}Al_x$ solid solutions crystallize in the rhombohedral Th_2Zn_{17} structure,[13] a structure which has consistently been found to be stoichiometric and free from disorder. The compositional dependence of the a and c lattice parameters is shown in Fig. 1.

The magnetic properties of the free particle samples were measured on a SQUID magnetometer between 5 and 300 K and on a Faraday magnetometer between 300 and 1000 K. The Curie temperatures were determined in small magnetic fields of ~0.1 T by plotting the square of the magnetization versus temperature and extrapolating the steepest part of the curve to zero magnetization.

The powder neutron diffraction patterns were collected at the University of Missouri Research Reactor by using a linear position sensitive diffractometer and neutrons with a wavelength of 1.4783 Å. The data for each sample were collected over ~24 h at both 295 and 10 K between 2θ angles of 5° and 105° on approximately 2 g of finely powdered sample placed in a thin wall vanadium container which was placed in a closed cycle refrigerator for the 10 K studies. Refinements of the neutron diffraction data were carried out with the FULLPROF[14] computer code which permits multiple phase refinement as well as magnetic structure refinement of each of the coexisting phases. The $Nd_2Fe_{17-x}Al_x$ solid solutions were found to contain ~3% or less by volume of α-iron.

The Mössbauer spectra were obtained at the University of Missouri-Rolla at 85 and 295 K on a constant-acceleration spectrometer which utilized a room temperature rhodium matrix cobalt-57 source and was calibrated at room temperature with α-iron foil. The Mössbauer absorbers, which were ~30 mg/cm^2, were prepared from powdered samples which had been sieved to a 0.045 mm or smaller particle diameter. The resulting spectra have been fit as discussed below and elsewhere[15] and the estimated errors are ±2 kOe for the weighted average maximum hyperfine fields and ±0.01 mm/s for the weighted average isomer shifts. At low aluminum contents, the Mössbauer spectra reveal the presence of between 2% and 3% by area of α-iron. The hyperfine parameters for this phase were constrained to their known values.

III. MAGNETIC STUDIES

The magnetization of the $Nd_2Fe_{17-x}Al_x$ solid solutions has been measured as a function of temperature in a 0.1 T field and the results for several of the compounds are shown in Fig. 2. From this figure it is immediately clear that the magnetization of $Nd_2Fe_{13}Al_4$ above ~350 K is much higher than that of Nd_2Fe_{17}, whereas, surprisingly, at ~350 K the magnetization of Nd_2Fe_{17} is similar to that of $Nd_2Fe_{11}Al_6$. As is explained in Sec. II, the temperature dependence of the magnetization has been used to determine the Curie temperatures of these solid solutions and its compositional dependence is shown in Fig. 3. The Curie temperature is at a maximum at an x value of approximately 3. A very similar variation of the Curie temperature with the aluminum content[10] in $Ho_2Fe_{17-x}Al_x$ and $Y_2Fe_{17-x}Al_x$ and the gallium content[9] in $Tb_2Fe_{17-x}Ga_x$ has recently been reported.

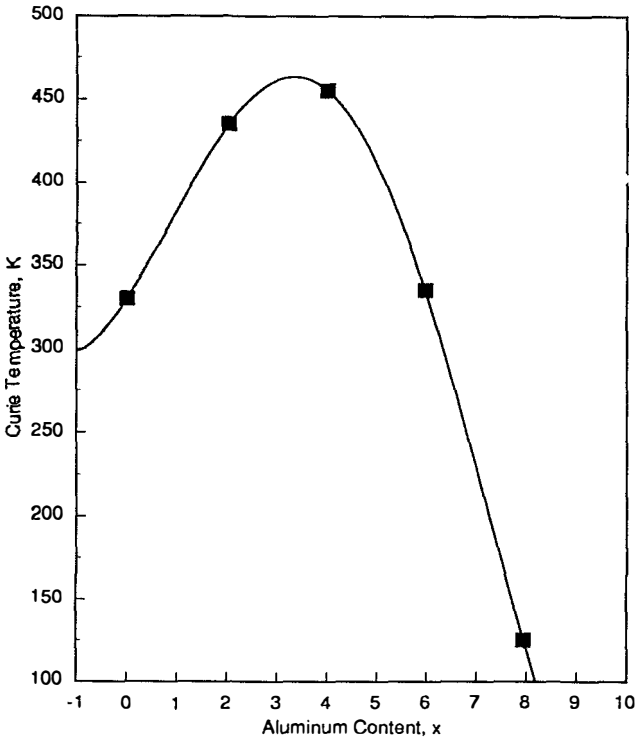

FIG. 3. The compositional dependence of the Curie temperature in the $Nd_2Fe_{17-x}Al_x$ solid solutions.

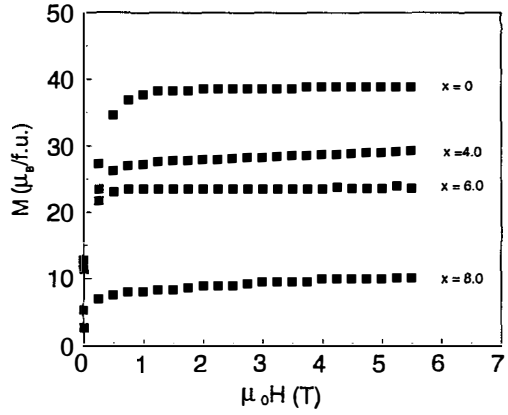

FIG. 4. The 4.2 K magnetization of several $Nd_2Fe_{17-x}Al_x$ solid solutions as a function of the applied fields.

It should be noted that the results shown in Fig. 2 were made in comparatively low magnetic fields in order to accurately determine the Curie temperatures. The applied fields of about 0.1 T are generally much smaller than the anisotropy fields present in the statistically oriented powder particles of the compounds investigated. Because the crystal field induced anisotropy is expected to vary strongly with temperature and composition, the increases and decreases in the temperature dependence of the magnetization observed at low temperature in Fig. 2 are probably artefacts and do not represent magnetic phase transitions. In order to compare the magnetizations in the different compounds and to further avoid such artefacts we have also performed magnetic measurements in high magnetic fields and the results are shown in Fig. 4. The saturation magnetization is at a maximum for Nd_2Fe_{17} as would be expected for the compound containing the most iron. The values of the saturation magnetization are virtually the same as those observed in the 10 K neutron diffraction study discussed below and given as the magnetic moment per formula unit in Table I.

IV. NEUTRON DIFFRACTION STUDIES

The results of the 295 K neutron diffraction measurements on the $Nd_2Fe_{17-x}Al_x$ solid solutions have previously been reported,[11] but in this earlier work the magnetic contributions to the neutron scattering were ignored. Herein we present complete refinements of both the nuclear and magnetic scattering at 10 and 295 K in Tables I and II, respectively. In order to provide a direct comparison with the $Nd_2Fe_{17-x}Al_x$ solid solutions, we have also remeasured[13] Nd_2Fe_{17} at 10 and 295 K. The results are also given in these tables. The 295 K aluminum occupancies, reported previously, deviate somewhat from the nominal compositions, with a fractional error of up to 15% for $Nd_2Fe_{15}Al_2$. In contrast, in the refinements reported in Table I, the 10 K aluminum occupancies were all within 0.1 of the nominal compositions except for our initial unconstrained refinement of the $Nd_2Fe_{15}Al_2$ data. In these initial refinements, a plot of the aluminum site occupancies as a function of composition followed reasonably smooth curves except for the 6*c* site in $Nd_2Fe_{15}Al_2$, for which the unconstrained 6*c* site occupancy of 9.6% was far too high. Because the 6*c* site is a low degeneracy site, and thus contributes relatively little to the overall scattering, small systematic errors may accumulate in its refinement and, hence, the deviation of the aluminum occupancy was not too surprising, especially at the low aluminum concentration in $Nd_2Fe_{15}Al_2$. To overcome this problem we have constrained the aluminum occupancy of the 6*c* site in $Nd_2Fe_{15}Al_2$ to 4%, as would be expected from the interpolated occupancy. All of the remaining aluminum occupancies in $Nd_2Fe_{15}Al_2$ have been refined and lead to a total aluminum occupancy of 2.03, or $Nd_2Fe_{14.97}Al_{2.03}$, a value which is completely consistent with the expected stoichiometry. The results in both Tables I and II use this constraint, but for all other compositions, the quoted occupancies are fully unconstrained.

A comparison of the occupancies given in Table I with our earlier room temperature results[11] shows generally excellent agreement, but the low temperature results should be viewed as more reliable, especially because of their excellent agreement with the highly accurate nominal compositions. As a result, the occupancies obtained from the 10 K neutron diffraction refinements have been used in the refinement of the 295 K data and to extract the magnetic moments given in Table II.

As is shown in Fig. 5, the aluminum almost completely avoids the 9*d* site, the site with the smallest Wigner–Seitz cell volume.[4] At compositions up to an x of approximately 6, aluminum prefers the 18*h* site and occupies the 6*c* and 18*f* site in an approximately random fashion. In contrast, at higher aluminum compositions, aluminum strongly prefers

TABLE I. The lattice and positional parameters, site occupancies, and moments in $Nd_2Fe_{17-x}Al_x$ as measured by neutron diffraction at 10 K.

Compound	Nd_2Fe_{17}	$Nd_2Fe_{15}Al_2$	$Nd_2Fe_{13}Al_4$	$Nd_2Fe_{11}Al_6$	$Nd_2Fe_9Al_8$	$Nd_2Fe_8Al_9$
x-refined	0.00	2.04	4.01	5.97	7.94	9.06
a, Å	8.5797(2)	8.6374(1)	8.6882(2)	8.7473(2)	8.8182(2)	8.8506(1)
c, Å	12.5021(2)	12.5728(3)	12.6579(3)	12.7399(3)	12.8042(4)	12.8486(2)
c/a	1.457	1.456	1.457	1.456	1.452	1.452
V, Å^3	797.0	812.3	827.5	844.2	862.3	871.6
Nd, 6c,z	0.3418(3)	0.3416(3)	0.3423(3)	0.3439(3)	0.3461(3)	0.3450(2)
Fe/Al, 6c,z	0.0951(3)	0.0955(2)	0.0957(2)	0.0968(3)	0.1019(4)	0.1024(4)
Fe/Al, 18f,x	0.2918(2)	0.2889(1)	0.2875(1)	0.2858(1)	0.2879(2)	0.2895(2)
Fe/Al, 18h,x	0.1687(2)	0.1689(1)	0.1705(1)	0.1707(1)	0.1695(2)	0.1692(1)
Fe/Al, 18h,z	0.4905(2)	0.4898(1)	0.4892(2)	0.4892(2)	0.4903(2)	0.4903(1)
%Al, 6c	0.0	4.0[a]	13.1(2)	43.1(3)	75.5(3)	97.6(4)
%Al, 9d	0.0	0.0	0.0	0.0	0.0	5.6(4)
%Al, 18f	0.0	7.0(2)	21.0(2)	38.6(3)	59.2(3)	74.0(3)
%Al, 18h	0.0	24.8(2)	41.4(2)	46.6(3)	47.8(3)	43.6(3)
R-factor	5.95	6.27	6.29	7.36	7.04	5.76
R_w-factor	7.81	8.24	8.17	9.37	9.08	7.31
R_m-factor	5.98	6.69	8.14	9.78	9.49	10.8
χ^2	3.77	3.24	3.55	3.82	2.71	1.77
μ, Nd, 6c, μ_B	2.9(2)	3.3(2)	3.0(1)	3.1(1)	1.9(2)	1.5(3)
μ, Fe, 6c, μ_B	3.5(2)	2.7(2)	1.9(3)	1.1(3)	1.0[a]	1.0[a]
μ, Fe, 9d, μ_B	2.5(2)	2.1(1)	1.2(2)	0.9(2)	0.7(3)	0.6(2)
μ, Fe, 18f, μ_B	2.9(2)	2.6(1)	2.0(2)	1.7(1)	0.5(2)	0.4(3)
μ, Fe, 18h, μ_B	2.3(2)	2.2(2)	1.7(1)	1.8(2)	0.5(2)	0.4(4)
μ/cell, μ_B	154.5	125.1	85.1	66.6	32.7	25.5
μ/formula, μ_B	51.5	41.7	28.4	22.2	10.9	8.5
α-Fe, vol %	0.0	3.00	2.13	0.44	0.63	1.06

[a]Parameter constrained to the value given.

the 6c and 18f sites and the aluminum occupancy of the 18h site remains relatively constant at approximately 45%. Very similar gallium and aluminum occupancy trends have been observed[9,16] in both $Tb_2Fe_{17-x}Ga_x$ and $Tb_2Fe_{17-x}Al_x$, but these occupancies do not agree well with those deduced earlier[8] from either an x-ray diffraction or a Mössbauer spectral study of $Nd_2Fe_{15}Al_2$. The trends in these occupancies may be understood, at least in part, on the basis of the near-neighbor environment of each site. The Wigner–Seitz[17] near neighbors and the 295 K cell volumes for Nd_2Fe_{17} are given in Table III. At low aluminum content, apparently because of the very short 6c–6c bond distance,[4,13] the aluminum avoids

TABLE II. The lattice and positional parameters, site occupancies, and moments in $Nd_2Fe_{17-x}Al_x$ as measured by neutron diffraction at 295 K.[a]

Compound	Nd_2Fe_{17}	$Nd_2Fe_{15}Al_2$	$Nd_2Fe_{13}Al_4$	$Nd_2Fe_{11}Al_6$	$Nd_2Fe_9Al_8$	$Nd_2Fe_8Al_9$
x-refined	0.00	2.04	4.01	5.97	7.94	9.06
a, Å	8.6002(1)	8.6569(1)	8.7112(2)	8.7615(2)	8.8306(2)	8.8676(2)
c, Å	12.4835(2)	12.5782(3)	12.6788(3)	12.7489(3)	12.8160(4)	12.8703(3)
c/a	1.452	1.453	1.456	1.455	1.451	1.451
V, Å^3	799.6	814.3	830.8	847.7	865.4	876.5
Nd, 6c, z	0.3426(3)	0.3427(3)	0.3429(3)	0.3435(3)	0.3451(2)	0.3458(2)
Fe/Al, 6c, z	0.0957(2)	0.0958(2)	0.0963(2)	0.0970(3)	0.1012(4)	0.1031(4)
Fe/Al, 18f, x	0.2882(1)	0.2874(1)	0.2862(1)	0.2869(2)	0.2875(2)	0.2909(2)
Fe/Al, 18h, x	0.1687(1)	0.1695(1)	0.1706(1)	0.1709(1)	0.1694(2)	0.1694(2)
Fe/Al, 18h, z	0.4893(1)	0.4895(1)	0.4898(2)	0.4893(2)	0.4905(2)	0.4899(2)
R-factor	5.48	4.40	4.83	4.84	5.35	5.39
R_w-factor	7.09	5.46	6.18	6.22	6.74	6.79
R_m-factor	6.22	3.41	7.01	6.64	...	...
χ^2	3.11	2.18	2.49	1.62	2.01	2.23
μ, Nd, 6c, μ_B	2.1(2)	2.9(1)	2.7(1)	0.32	...	...
μ, Fe, 6c, μ_B	2.5(2)	2.5(2)	1.8(3)	0.74	...	...
μ, Fe, 9d, μ_B	1.7(2)	2.2(1)	1.2(2)	0.74	...	...
μ, Fe, 18f, μ_B	2.4(2)	2.4(1)	2.0(2)	0.74	...	...
μ, Fe, 18h, μ_B	1.7(2)	2.1(2)	1.5(1)	0.74	...	...
μ/cell, μ_B	116.7	120.2	80.6	26.4	...	...
μ/formula, μ_B	38.9	40.1	26.9	8.8	...	...
α-Fe, vol %	0.0	3.0	2.13	0.44	0.63	1.06

[a]The site occupancies are the same as those given in Table I.

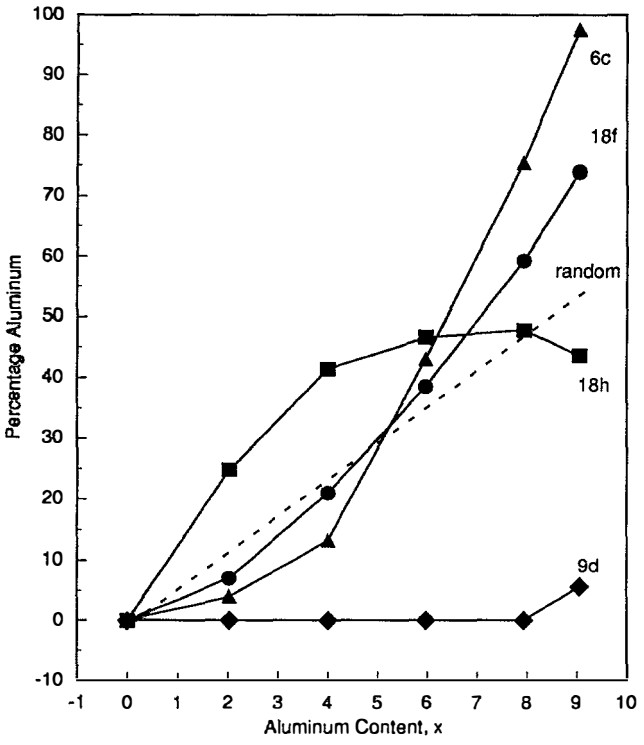

FIG. 5. The percentage aluminum found on each of the four crystallographic iron sites in the $Nd_2Fe_{17-x}Al_x$ solid solutions. The dashed line represents random occupation by aluminum.

the 6*c* site even though this site has the largest Wigner–Seitz cell volume.

At high aluminum content, aluminum prefers the 6*c* site because this site has the largest number of 9*d* near neighbors and, in this way, the number of aluminum near-neighbor pairs are minimized. At low aluminum content, the aluminum occupancy of the 18*h* site is approximately twice the random occupation. It is relatively easy to understand why there is such a strong preference of aluminum or gallium for the 18*h* site at low content. As may be seen in Table III, the 18*h* site is exceptional in that it has three rare-earth near neighbors. If one bears in mind that the heat of mixing between neodymium and iron is close to zero, whereas that of neodymium and aluminum is highly negative, it is clear that the 18*h* site will be strongly favored by aluminum.[18] A similar preference for silicon to associate with rare-earth near neighbors has been observed[19,20] in $Nd_2Fe_{14-x}Si_xB$ and $Y_2Fe_{14-x}Si_xB$.

In Nd_2Fe_{17} it should be noted that, interestingly, the *c*-lattice parameter is larger at 10 K than at 295 K. A similar result has been reported[21] for Y_2Fe_{17} and associated with magnetostriction at the magnetic ordering temperature, a magnetostriction which predominately occurs along the *c* axis. The increase in the *c*-lattice parameter at low temperature is apparently a reflection of the 'invar' effect, an effect which is less pronounced in the aluminum solid solutions because of their increased Curie temperatures, see Fig. 3. In order to confirm this observation, a detailed neutron diffraction study of Nd_2Fe_{17} as a function of temperature, is currently in progress.

At 10 and 295 K the neutron diffraction derived lattice parameters and unit cell volume increase linearly with increasing aluminum content. The 295 K values are virtually the same as those obtained by x-ray diffraction and shown in Fig. 1. At 295 K the unit cell volume increases by 8.5 Å^3 per aluminum whereas at 10 K the change is slightly reduced to 8.3 Å^3 per aluminum. This behavior is similar to that observed[16] in $Tb_2Fe_{17-x}Al_x$ but differs from that observed[9] in $Tb_2Fe_{17-x}Ga_x$. In the latter compounds, although the unit cell volume increases linearly with increasing gallium content, the lattice parameters increase linearly only at lower gallium content and, from an x of 5 to 8, the *c* lattice parameter becomes approximately constant. The *c*/*a* ratio, as a function of aluminum content, is interesting because it both shows a maximum at an x of 4, a maximum similar to that found[9] in $Tb_2Fe_{17-x}Ga_x$, and a substantial increase between 295 and 10 K.

The compositional dependences of the magnetic moment on each site in the $Nd_2Fe_{17-x}Al_x$ solid solutions at 10 and 295 K are shown in Figs. 6(A) and 6(B) respectively. The room temperature refinements show no magnetic order for an aluminum content above x equal to 6, but the 10 K data, as shown in Fig. 6(A) reveal magnetic ordering persisting to the limit of the aluminum solubility at x equal to 9. As shown in Fig. 6(B) the moments for $Nd_2Fe_{15}Al_2$ at 295 K are all either the same or larger than in Nd_2Fe_{17}. The increase is most pronounced for the neodymium moment which is $0.8\mu_B$ larger, or at least $0.6\mu_B$ larger if one considers the errors on the moments, in the former compound. Because the rare-earth moments saturate more slowly than the iron moments with decreasing temperature, it is not surprising that they are also sensitive to the presence of aluminum and to the increase in the Curie temperature between Nd_2Fe_{17} and $Nd_2Fe_{15}Al_2$. The bulk magnetic moment decreases with increasing x, both because of the decreasing iron content and

TABLE III. The 295 K Wigner–Seitz cell volumes and near neighbors in Nd_2Fe_{17}.

Site	Number of near neighbors					Total No. Iron nn	Wigner–Seitz cell volume, Å^3
	Nd 6*c*	Fe 6*c*	Fe 9*d*	Fe 18*f*	Fe 18*h*		
Nd 6*c*	1	1	3	6	9	19	31.85
Fe 6*c*	1	1	3	6	3	13	12.43
Fe 9*d*	2	2	0	4	4	10	11.33
Fe 18*f*	2	2	2	2	4	10	11.84
Fe 18*h*	3	1	2	4	2	9	12.16

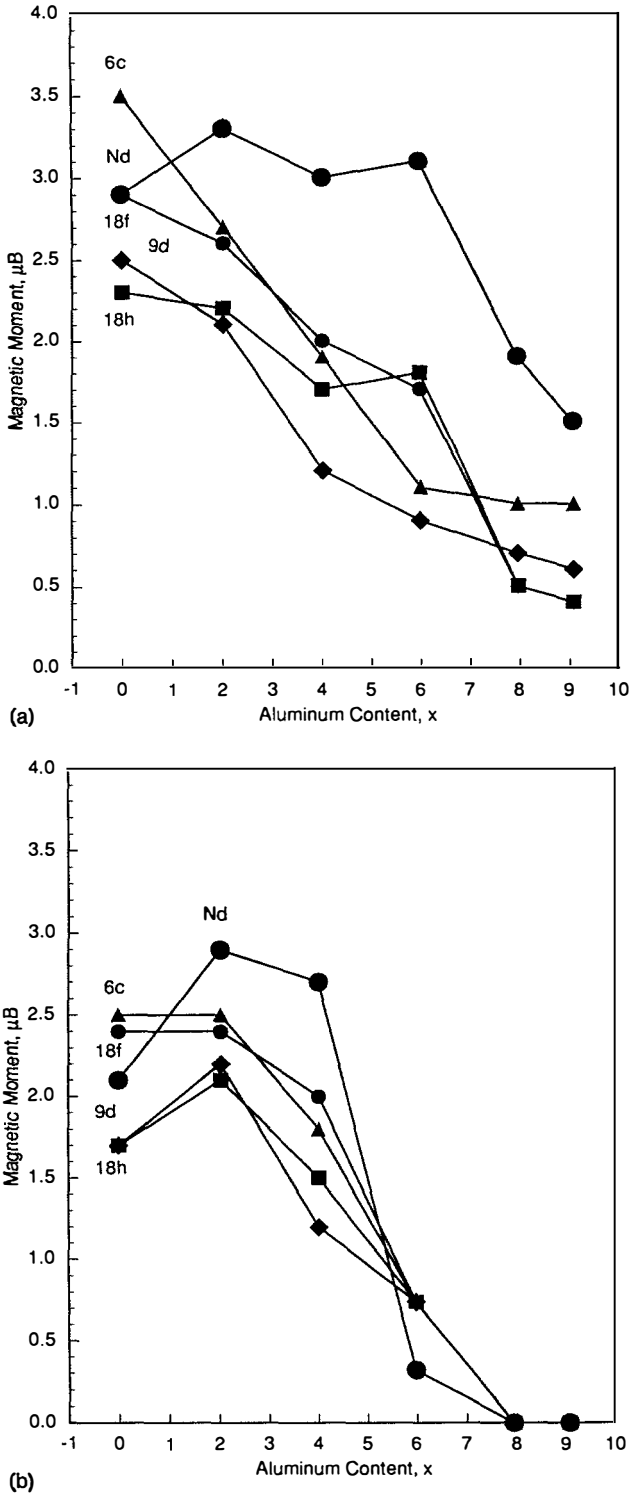

FIG. 6. The iron and neodymium magnetic moments in the $Nd_2Fe_{17-x}Al_x$ solid solutions measured at (A) 10 K and at (B) 295 K. The iron $6c$ site is given by ▲, the $9d$ site by ◆, the $18f$ site by ●, the $18h$ site by ■, and the neodymium $6c$ site by ●.

because of the reduction in the ordered moments on the remaining iron atoms, see Table I.

For $Nd_2Fe_{15}Al_2$, which is just below the maximum Curie point aluminum composition, the iron moments at 10 K are quite large, averaging $2.34\mu_B$ per iron, and yield a bulk moment of $41.7\mu_B$ per formula unit. It appears that the enhanced exchange between the remaining iron atoms more than compensate for the reduced number of exchange paths at this composition. The changes in slope observed for the neodymium and iron $18f$ and $18h$ moments at 10 K for $Nd_2Fe_{11}Al_6$, see Fig. 6(A), appear to be real as a refinement with lower moments resulted in a significantly poorer fit.

The values of the magnetic moments per formula unit, derived from the 10 K neutron diffraction data, see Table I, are in excellent agreement with the 4.2 K values of the saturation magnetization shown in Fig. 4. In contrast, at 10 K the $41.7\mu_B$ saturation magnetic moment per formula unit, reported in Table I for $Nd_2Fe_{15}Al_2$, is substantially higher than the 5 K value of $32.8\mu_B$ reported earlier.[8]

V. MÖSSBAUER SPECTRAL STUDIES

Of the four crystallographically distinct iron sites in the rhombohedral Nd_2Fe_{17} structure,[13] the $9d$, $18f$, and $18h$ sites split[4,22,23] into two magnetically inequivalent sites because of their point symmetries and the basal orientation of the magnetization. Consequently, the Mössbauer spectra of the $Nd_2Fe_{17-x}Al_x$ solid solutions were initially fit with seven broadened magnetic sextets. The Mössbauer spectra show that the long range magnetic ordering in these compounds becomes negligible at 85 K for x greater than 8, and at 295 K for x greater than 6. These x values are in agreement with the magnetic neutron scattering discussed above. In these preliminary Mössbauer spectral fits, the area weighted average magnetic hyperfine field at 85 K decreases by approximately 20 kOe per aluminum. In contrast, at 295 K it increases with increasing aluminum content up to an x value of 2 and then decreases for higher aluminum content.[11] The occurrence of this maximum may be explained by the strongly concentration dependent Curie temperature which gives rise to a similar maximum in this concentration range, see Fig. 3.

In the above preliminary fits, all iron atoms on a specific lattice site were assumed to have the same hyperfine parameters independent of the number of aluminum atoms in their near-neighbor environment. However, in $Nd_2Fe_{17-x}Al_x$ the near-neighbor environment of a particular iron atom is influenced by the presence of aluminum. The variation in the near-neighbor environment for a specific iron site produces a distribution of the hyperfine parameters of this site. By assuming that aluminum is substituted randomly on the $6c$, $18f$, and $18h$ sites, with the site occupancies given in Table I, a binomial distribution of the aluminum near neighbors at a specific iron site can be calculated. Figure 7 shows the percentage of the site which has a given number of aluminum near neighbors for the four crystallographic sites in $Nd_2Fe_{15}Al_2$ and $Nd_2Fe_{11}Al_6$. Figure 7(A) indicates that in $Nd_2Fe_{15}Al_2$ the most probable environments for an iron atom contain one or two aluminum near neighbors. In contrast, Fig. 7(B) indicates that in $Nd_2Fe_{11}Al_6$ the most probable environments for an iron atom contain from 2 to 6 aluminum atoms. This change in distribution can be seen in the lineshape of the individual components of the distribution fits shown in Fig. 8.

The magnetically ordered Mössbauer spectra were fit with a model which takes into account the binomial distribu-

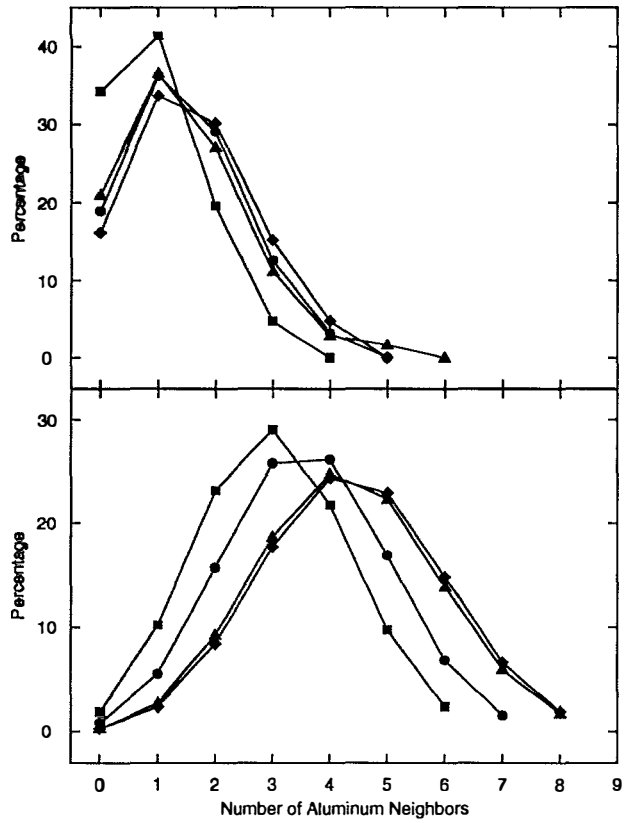

FIG. 7. The percentage of a given site which has a specific number of aluminum near neighbors for $Nd_2Fe_{15}Al_2$, top, and $Nd_2Fe_{11}Al_6$, bottom. The $6c$ site is given by ▲, the $9d$ site by ◆, the $18f$ site by ●, and the $18h$ site by ■.

tion of near neighbor environments.[19,23] In this fitting procedure, the iron atoms on a specific crystallographic site are represented by several magnetic sextets, each sextet resulting from the iron atoms having a different number of aluminum near neighbors. The relative area of these sextets is determined from the binomial distribution. Both the maximum hyperfine field, H_{max}, for the iron atoms on a specific site which have zero aluminum near neighbors, and a decremental field, ΔH, the change in the hyperfine field when one aluminum replaces an iron atom in the near-neighbor environment of the site, have been determined. In this approach,[19,23] for a specific aluminum concentration, x, the magnetic hyperfine field, $H(x,n)$, at an iron atom with n aluminum near neighbors is given by $H(x,n) = H_{max}(x) - n\Delta H(x)$. The initial values for the isomer shifts and the quadrupole shifts were taken from the preliminary fits mentioned above which used broadened sextets.

The binomial distribution fits of the Mössbauer spectra of $Nd_2Fe_{17-x}Al_x$, measured at 85 K, are shown in Fig. 8. The hyperfine parameters derived from these binomial fits of the spectra measured at 295 and 85 K are given in Tables IV and V, respectively. The dependence of H_{max} on the aluminum content for different sites at 85 and 295 K is shown in Fig. 9. The area weighted average values of H_{max}, ΔH, and the isomer shift are shown in Fig. 10. As indicated at the bottom of Fig. 10, the area weighted average isomer shift

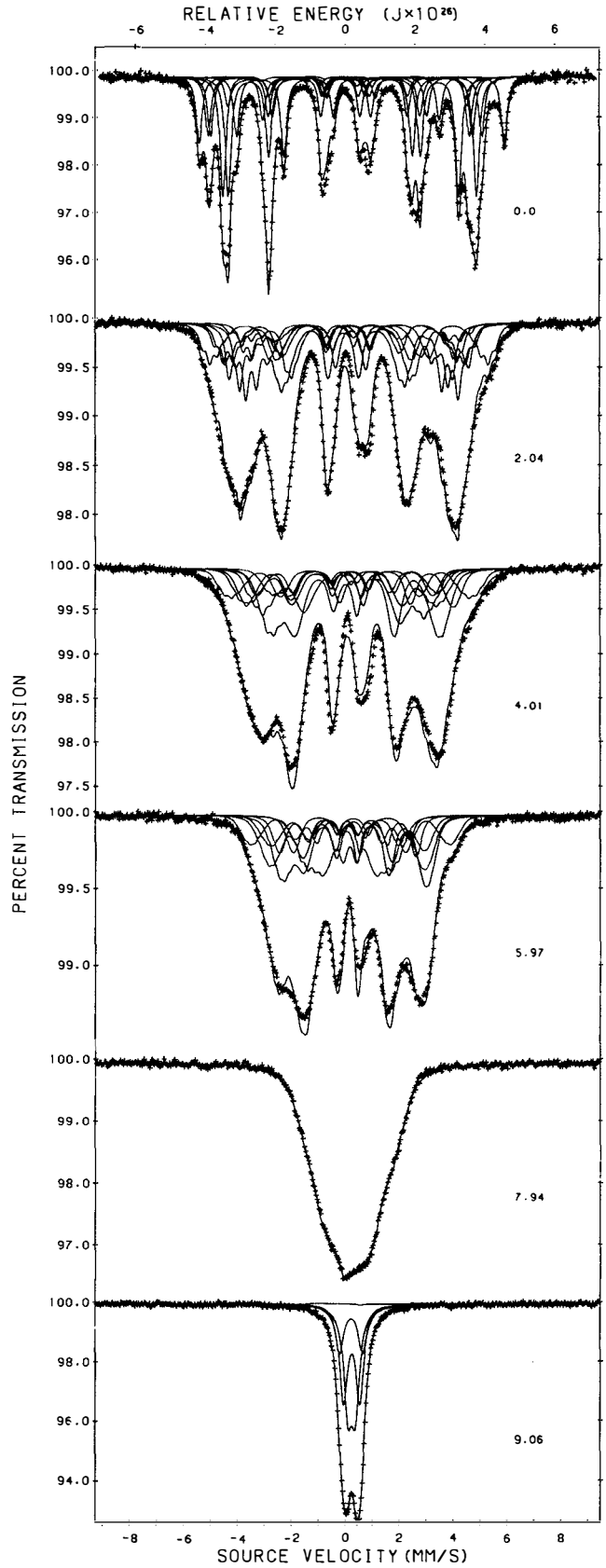

FIG. 8. The Mössbauer spectra of the $Nd_2Fe_{17-x}Al_x$ solid solutions obtained at 85 K and fit with a binomial distribution of aluminum atoms in the near-neighbor environment of each iron site.

TABLE IV. Mössbauer spectral parameters for $Nd_2Fe_{17-x}Al_x$ obtained at 295 K.

Parameter	x	Site 6c	$9d_6$	$9d_3$	$18f_{12}$	$18f_6$	$18h_{12}$	$18h_6$	Wt. avg.
H_{max} (kOe)	0.00	186	175	150	151	153	151	141	157
	2.04	261	234	210	219	208	209	205	221
	4.01	249	215	185	205	194	173	167	199
	5.97	...	...	...	...	...	...	...	79
ΔH (kOe)	2.04	12.2	12.6	6.0	23.9	15.1	22.0	17.0	17.7
	4.01	10.2	11.0	8.4	17.0	9.8	19.0	13.0	13.3
δ (mm/s)[a]	0.00	0.110	−0.165	−0.165	−0.090	−0.090	−0.064	−0.064	−0.071
	2.04	0.150	−0.153	−0.153	−0.040	−0.040	−0.051	−0.051	−0.042
	4.01	0.140	−0.120	−0.120	−0.030	−0.030	−0.036	−0.036	−0.027
	5.97	...	...	...	...	...	...	...	0.036
	7.94	0.225	0.086	...	0.084	...	0.081	...	0.092
	9.06	0.230	0.113	...	0.117	...	0.120	...	0.118
QS (mm/s)	0.00	0.00	−0.12	0.32	0.37	0.00	−0.44	0.45	...
	2.04	0.00	0.03	0.47	0.25	−0.12	−0.33	0.56	...
	4.01	−0.02	0.07	0.52	0.22	−0.14	−0.26	0.62	...
ΔE_Q (mm/s)	7.94	0.31	0.59	...	0.81	...	0.30	...	0.53
	9.06	0.35	0.57	...	0.98	...	0.20	...	0.56

[a]Relative to α-iron foil at 295 K.

increases with increasing aluminum content. Similar increases have been observed previously[16,24,25] and may be attributed to interatomic charge transfer and intraatomic iron $4s-3d$ charge redistribution in the presence of substitutional atoms such as aluminum and gallium.

In a Mössbauer study of binary iron-aluminum alloys, Stearns[26,27] deduced an increase in isomer shift of 0.03 mm/s per aluminum in the near neighbor environment of iron. If we assume that, on average, for $Nd_2Fe_{15}Al_2$, the iron atoms have one aluminum near neighbor, as shown in Fig. 7(A) the observed increase in weighted average isomer shift of ~0.02 mm/s, shown in Fig. 10, is very similar to that observed by Stearns.[26,27] Furthermore, in $Nd_2Fe_{11}Al_6$, as shown in Fig. 7(B) on average the iron atoms have four aluminum near neighbors and an increase in weighted average isomer shift of ~0.12 mm/s is observed, see Fig. 10. We can thus con-

TABLE V. Mössbauer spectral parameters for $Nd_2Fe_{17-x}Al_x$ obtained at 85 K.

Parameter	x	Site 6c	$9d_6$	$9d_3$	$18f_{12}$	$18f_6$	$18h_{12}$	$18h_6$	Wt. avg.
H_{max} (kOe)	0.00	352	301	275	285	315	271	267	291
	2.04	338	290	265	269	300	257	249	281
	4.01	307	252	220	230	269	220	215	243
	5.97	255	204	165	193	216	145	145	189
	7.94	...	...	...	...	...	...	...	63
ΔH (kOe)	2.04	17.3	19.4	20.0	24.8	22.2	25.7	19.8	21.5
	4.01	14.0	17.0	13.7	15.0	12.1	18.0	16.0	15.4
	5.97	12.0	11.7	9.5	11.6	8.0	16.0	12.0	11.7
δ (mm/s)[a]	0.00	0.250	−0.070	−0.070	0.060	0.060	0.064	0.064	0.061
	2.04	0.152	−0.027	−0.027	0.103	0.103	0.025	0.025	0.059
	4.01	0.180	−0.044	−0.044	0.139	0.139	0.068	0.068	0.081
	5.97	0.230	0.040	0.040	0.140	0.140	0.084	0.084	0.124
	7.94	...	...	...	...	...	...	...	0.207
	9.06	0.250	0.237	...	0.222	...	0.243	...	0.237
QS (mm/s)	0.00	−0.05	−0.10	0.34	0.44	−0.10	−0.42	0.48	...
	2.04	−0.03	−0.25	0.18	0.48	−0.10	−0.39	−0.51	...
	4.01	−0.01	−0.20	0.23	0.42	−0.11	−0.32	−0.57	...
	5.97	−0.17	0.00	0.44	0.31	−0.23	−0.42	−0.47	...
ΔE_Q (mm/s)	9.06	0.048	0.603	...	0.848	...	0.273	...	0.519

[a]Relative to α-iron foil at 295 K.

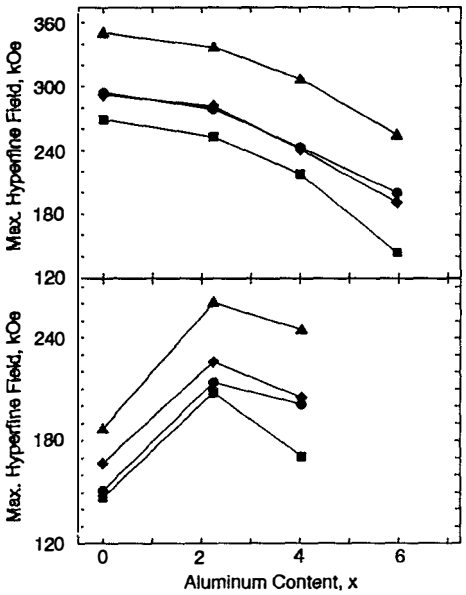

FIG. 9. The 85 K, top, and 295 K, bottom, compositional dependence of the site weighted average maximum hyperfine fields, H_{max}, in $Nd_2Fe_{17-x}Al_x$. The $6c$ site is given by ▲, the $9d$ site by ◆, the $18f$ site by ●, and the $18h$ site by ■.

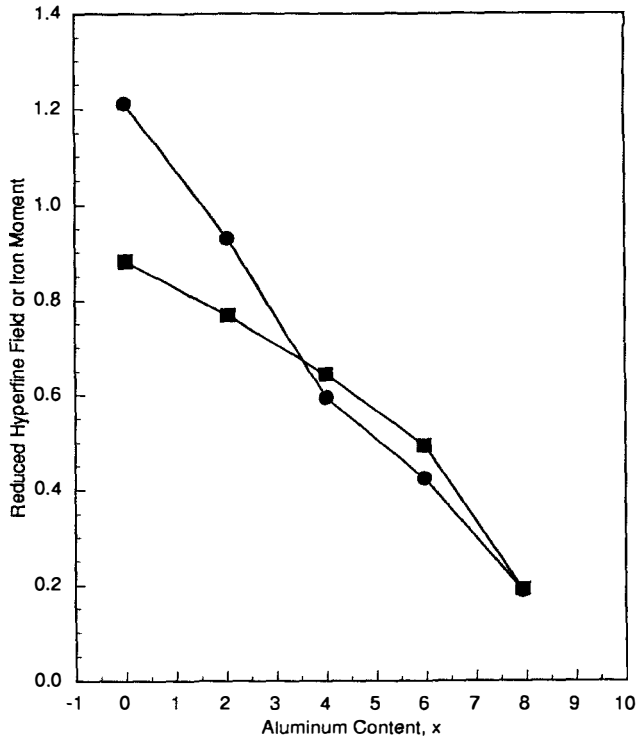

FIG. 11. The α-iron foil normalized $Nd_2Fe_{17-x}Al_x$ 85 K average hyperfine fields, ■, and 10 K average magnetic moments, ●, as a function of aluminum content.

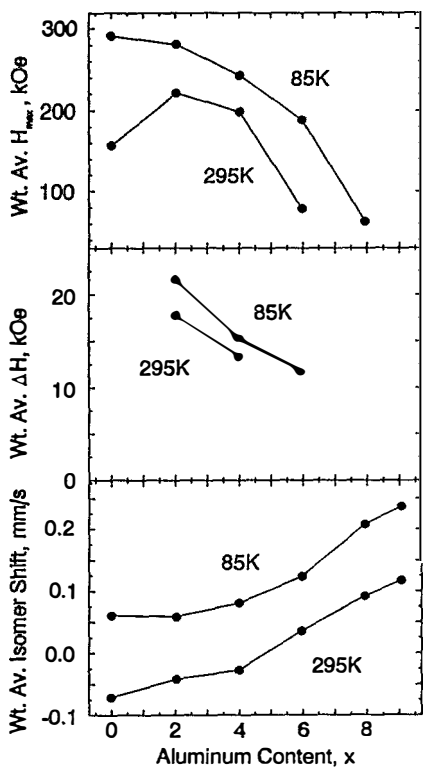

FIG. 10. The 295 and 85 K compositional dependence of the weighted average maximum hyperfine field, H_{max}, the weighted average ΔH, and the weighted average isomer shift as a function of aluminum content in $Nd_2Fe_{17-x}Al_x$.

clude that aluminum has the same influence on the isomer shift in the binary alloys and in the $Nd_2Fe_{17-x}Al_x$ solid solutions.

For all iron sites, H_{max} at 85 K decreases uniformly with increasing aluminum content and the area weighted average value of H_{max} decreases by 17 kOe/Al. At 295 K the area weighted average value of H_{max} for $Nd_2Fe_{15}Al_2$ is 63 kOe higher than in Nd_2Fe_{17} but H_{max} decreases with increasing aluminum content for compounds with x above 4. Of course, this higher H_{max} value at 295 K arises in part because of the maximum in the Curie temperature observed at an x of approximately four, as is shown in Fig. 3. At 85 K this increase is not expected because 85 K is well below the Curie temperature for all the compounds. The 85 K weighted average ΔH is in the range of 6%–7% of the weighted average of H_{max} and decreases from 22 to 12 kOe as the aluminum content increases from 2.04 to 5.97.

VI. DISCUSSION

It is useful to compare the Mössbauer results described above with those obtained for binary iron-aluminum alloys by Stearns.[26,27] A plot of the 85 K average hyperfine fields in $Nd_2Fe_{17-x}Al_x$, normalized to the field in α-iron, is given as a function of aluminum content in Fig. 11. This figure also shows the 10 K average magnetic moments in $Nd_2Fe_{17-x}Al_x$, see Table I, normalized to the moment in α-iron. A similar plot was shown by Stearns[27] for the binary iron-aluminum alloys with aluminum concentrations up to 15 at. %, a concentration which corresponds to an x of 2.55 in $Nd_2Fe_{17-x}Al_x$. In agreement with Stearns,[27] over the range

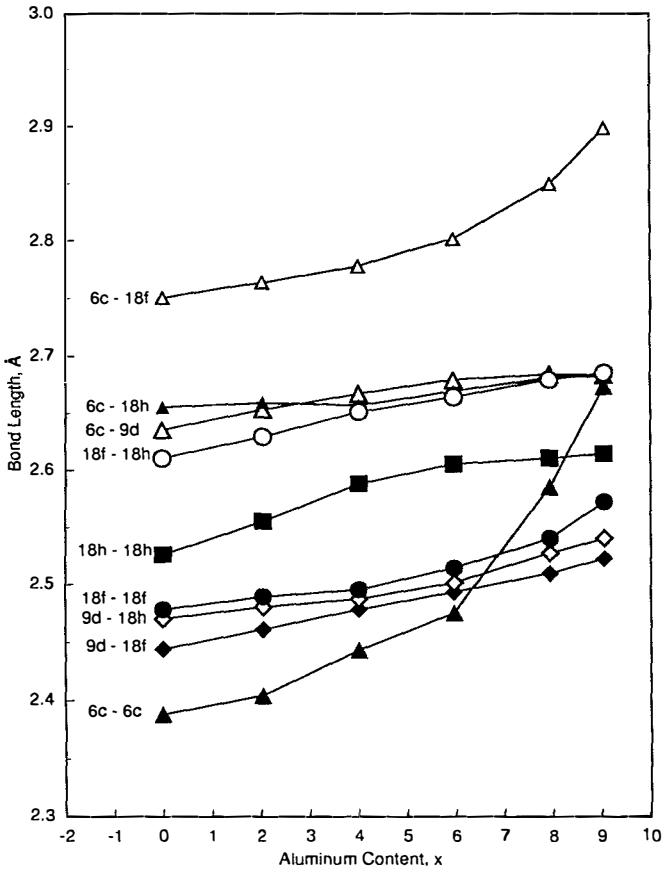

FIG. 12. The iron-iron bond lengths as a function of aluminum content in the $Nd_2Fe_{17-x}Al_x$ solid solutions.

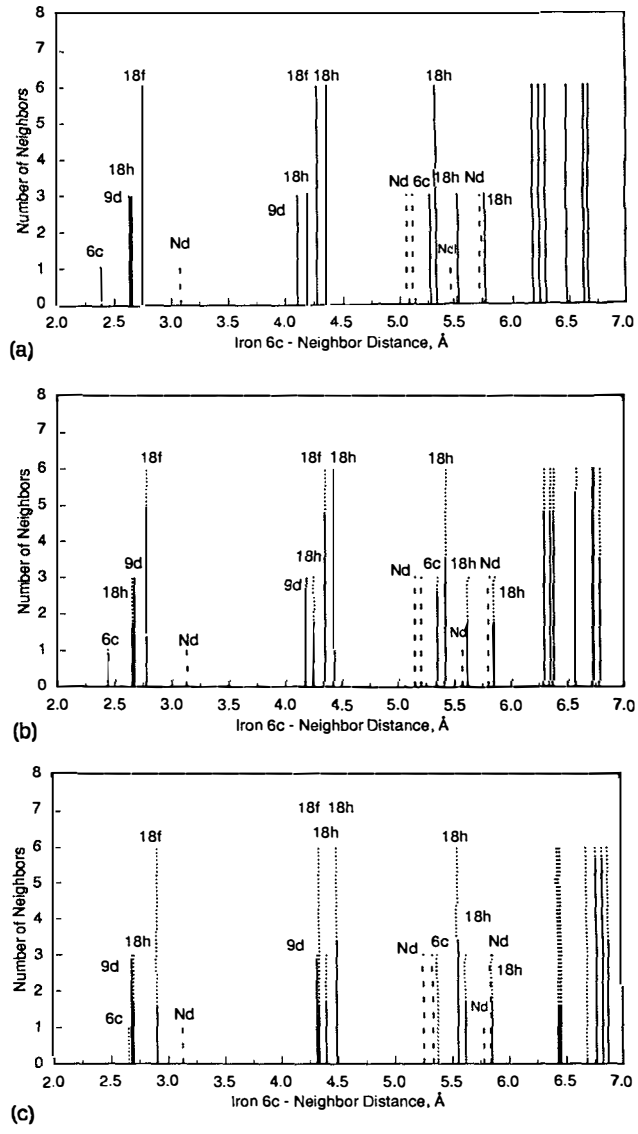

FIG. 13. A plot of the number of neighbors as a function of distance in (A) Nd_2Fe_{17}, (B) $Nd_2Fe_{13}Al_4$, and (C) $Nd_2Fe_8Al_9$. The solid, dotted, and dashed lines represent the number of iron, aluminum, and neodymium neighbors, respectively.

$0<x<2.55$ the normalized hyperfine field is smaller than the normalized magnetic moment. In contrast, for x above three, the normalized hyperfine fields and magnetic moments show a very similar decrease with increasing aluminum content. This decrease indicates that the two quantities are rather equivalent and probe the magnetic interactions in a similar fashion. Furthermore, at high aluminum content, the aluminum atoms seem to have a long range effect on the magnetic interactions in the lattice, whereas at low aluminum concentration, as noted by Stearns,[27] the aluminum atoms act as isolated magnetic holes in the lattice.

In the same study, Stearns[27] observed a ΔH value of $\sim 7\%$ of $H_{\max}$, a value which is very similar to those observed herein for the $Nd_2Fe_{17-x}Al_x$ solid solutions. In contrast with our observations, see Fig. 10, Stearns found that in this aluminum concentration range, $H_{\max}$ and ΔH show little or no compositional dependence. However, for aluminum concentrations greater than 15 at. %, she reported[26] a decrease in $H_{\max}$ with increasing aluminum concentration. One has to be cautious in comparing Stearns[26,27] results with our results, because her model to fit the Mössbauer spectra takes into account aluminum atoms not only in the first near-neighbor shell but also in the subsequent four shells. In contrast, because of the increased number of crystallographic iron sites in Nd_2Fe_{17}, our model takes into account only the first near-neighbor shell. The decrease in $H_{\max}$ and ΔH with increasing aluminum content shown in Fig. 10, may be due to the presence of an increasing number of aluminum atoms in the second and subsequent neighbor shells of the iron atom. Indeed, the magnetic interactions, both in several binary iron alloys[27,28] and in the $Dy_2Fe_{17-x}Al_x$ solid solutions,[29] have been interpreted within the Friedel model. In particular, the effect of the impurity atom on the iron hyperfine field shows an oscillatory behavior as a function of the distance between the iron atom and its subsequent shells of neighbors. These oscillations are known as Friedel oscillations and are similar to the RKKY oscillations.

Because the unit cell of the $Nd_2Fe_{17-x}Al_x$ solid solutions expands with increasing aluminum content, the iron-iron bond distances increase, as shown in Fig. 12, an increase which is especially pronounced for the $6c-6c$ and $6c-18f$

bond distances. As a consequence, the average distance between an iron atom and its subsequent neighbor shells increases, as is shown in Fig. 13 for the $6c$ iron site in Nd_2Fe_{17}, $Nd_2Fe_{13}Al_4$, and $Nd_2Fe_8Al_9$. Simultaneously, the wavelength of the Friedel oscillation increases with aluminum content and, hence, the ratio of the wavelength to the shell distance may become more favorable for ferromagnetic exchange. Therefore, it is possible that the contribution to the hyperfine field of aluminum in the second shell, between 4 and 4.5 Å, becomes more positive with increasing x and results in a decrease in ΔH, see Fig. 10. This would also account for the increase observed in the Curie temperature for x values between 0 and 4. However, the situation is more complex in view of the recent results obtained[12,30] for $Nd_2Fe_{17-x}Si_x$ and $Ce_2Fe_{17-x}Si_x$. These results indicate that increasing x leads to an increase in the Curie temperature, as in the $Nd_2Fe_{17-x}Al_x$ solid solutions. However, in the two silicon solid solutions, this Curie temperature increase is accompanied by a decrease in the unit cell volume rather than by an increase, as in the aluminum solid solutions.

In a more recent study of iron-aluminum alloys, with an aluminum content of 27%, Fultz *et al.*[31] have used a different approach to fit the Mössbauer spectra of these alloys. In their model, ΔH varies with the number of aluminum near neighbors in the first shell, and the effect of the subsequent shells is not taken into account. For one aluminum near neighbor, ΔH is ~15 kOe and increases up to 50 kOe for the sixth aluminum near neighbor in the first shell.

Thus, it is difficult to interpret the compositional dependence of H_{max} and ΔH shown in Fig. 10, because clearly the aluminum dependence, especially in ΔH, may be inherent in the model used to fit the data. More elaborate models including the second near-neighbor shell or a variable ΔH, could be used but are very difficult to implement because of the complexity of the $Nd_2Fe_{17-x}Al_x$ crystallographic structure.

ACKNOWLEDGMENTS

The authors acknowledge, with thanks, NATO for a cooperative scientific research grant (92-1160), the Division of Materials Research of the US National Science Foundation, for grant DMR-9214271, and the University of Missouri Research Board for financial support of the neutron diffraction work. GJL would like to thank the Commission for Educational Exchange between the United States of America, Belgium, and Luxembourg for a Fulbright Research Fellowship during the 1993-1994 academic year. DPM would like to thank the Dutch Foundation of Fundamental Research on Matter, for their financial support.

[1] D. B. de Mooij and K. H. J. Buschow, J. Less-Common Met. **142**, 349 (1988).
[2] J. M. D. Coey and H. Sun, J. Magn. Magn. Mater. **87**, L251 (1990).
[3] H. Sun, J. M. D. Coey, Y. Otani, and D. P. F. Hurley, J. Phys. Condens. Matter **2**, 6465 (1990).
[4] G. J. Long, O. A. Pringle, F. Grandjean, and K. H. J. Buschow, J. Appl. Phys. **72**, 4845 (1992).
[5] G. J. Long, O. A. Pringle, F. Grandjean, W. B. Yelon, and K. H. J. Buschow, J. Appl. Phys. **74**, 504 (1993).
[6] G. J. Long, O. A. Pringle, F. Grandjean, and K. H. J. Buschow, J. Appl. Phys. **75**, 2598 (1994).
[7] K. H. J. Buschow, in *Supermagnets, Hard Magnetic Materials*, edited by G. J. Long and F. Grandjean (Kluwer, Dordrecht, 1991), p. 553.
[8] F. Weitzer, K. Hiebl, and P. Rogl, J. Appl. Phys. **65**, 4963 (1989); B. P. Hu and J. M. D. Coey, J. Less-Common Metals **142**, 295 (1988).
[9] Z. Hu, W. B. Yelon, S. Mishra, G. J. Long, O. A. Pringle, D. P. Middleton, K. H. J. Buschow, and F. Grandjean, J. Appl. Phys. **76**, 443 (1994).
[10] T. H. Jacobs, K. H. J. Buschow, G. F. Zhou, X. Li, and F. R. de Boer, J. Magn. Magn. Mater. **116**, 220 (1992); T. H. Jacobs, K. H. J. Buschow, G. F. Zhou, and F. R. de Boer, Physica B **179**, 177 (1992); D. P. Middleton and K. H. J. Buschow, J. Alloys Comp. **203**, 217 (1994).
[11] W. B. Yelon, H. Xie, G. J. Long, O. A. Pringle, F. Grandjean, and K. H. J. Buschow, J. Appl. Phys. **73**, 6029 (1993).
[12] G. J. Long, G. K. Marasinghe, S. Mishra, O. A. Pringle, F. Grandjean, K. H. J. Buschow, D. P. Middleton, W. B. Yelon, F. Pourarian, and O. Isnard, Solid State Commun. **88**, 761 (1993).
[13] J. F. Herbst, J. J. Croat, R. W. Lee, and W. B. Yelon, J. Appl. Phys. **53**, 6029 (1982).
[14] FULLPROF Reitveld refinement written code by J. Rodriguez-Carjaval, Institute Laue Langevin, Grenoble, France.
[15] G. J. Long and F. Grandjean, in *Supermagnets, Hard Magnetic Materials*, edited by G. J. Long and F. Grandjean (Kluwer, Dordrecht, 1991), p. 355.
[16] G. K. Marasinghe, S. Mishra, O. A. Pringle, G. J. Long, Z. Hu, W. B. Yelon, F. Grandjean, D. P. Middleton, and K. H. J. Buschow, J. Appl. Phys. (to be published).
[17] L. Gelato, J. Appl. Crystallogr. **14**, 141 (1981).
[18] A. R. Niessen, F. R. de Boer, R. Boom, P. F. de Châtel, W. C. M. Mattens, and A. R. Miedema, Calphad **7**, 51 (1983).
[19] G. K. Marasinghe, O. A. Pringle, G. J. Long, W. J. James, D. Xie, J. Li, W. B. Yelon, and F. Grandjean, J. Appl. Phys. **74**, 6798 (1993).
[20] G. K. Marasinghe, O. A. Pringle, G. J. Long, W. B. Yelon, and F. Grandjean, J. Appl. Phys. **76**, 2960 (1994).
[21] A. V. Andreev, F. R. de Boer, T. H. Jacobs, and K. H. J. Buschow, Physica **175B**, 361 (1991).
[22] P. C. M. Gubbens, J. J. Van Loef, and K. H. J. Buschow, J. Physique, Coll. C6, **35**, 617 (1974).
[23] G. J. Long and F. Grandjean, in *Interstitial Alloys for Reduced Energy Consumption and Pollution*, edited by F. Grandjean, G. J. Long and K. H. J. Buschow (Kluwer, Dordrecht, in press).
[24] A. M. van der Kraan and K. H. J. Buschow, Physica **138B**, 55 (1986).
[25] J. W. C. de Vries, R. C. Thiel, and K. H. J. Buschow, J. Phys. F **15**, 2403 (1985).
[26] M. B. Stearns, J. Appl. Phys. **35**, 1095 (1964).
[27] M. B. Stearns, Phys. Rev. **147**, 439 (1966).
[28] M. B. Stearns, Phys. Rev. B **4**, 4069 (1971).
[29] D. Plusa, R. Pfranger, and B. Wyslocki, J. Less-Common Metals **99**, 87 (1984).
[30] D. P. Middleton and K. H. J. Buschow, J. Alloys Compounds **203**, 217 (1994).
[31] B. Fultz, Z. Q. Gao, and H. Hamdeh, Hyperfine Interactions **54**, 521 (1990).